

# Water Resources Research®

## RESEARCH ARTICLE

10.1029/2022WR032295

## Quantifying the Impact of Lagged Hydrological Responses on the Effectiveness of Groundwater Conservation

Thomas J. Glose<sup>1</sup> , Sam Zipper<sup>1</sup> , David W. Hyndman<sup>2,3</sup> , Anthony D. Kendall<sup>3</sup> ,  
Jillian M. Deines<sup>4</sup> , and James J. Butler Jr.<sup>1</sup> 

<sup>1</sup>Kansas Geological Survey, University of Kansas, Lawrence, KS, USA, <sup>2</sup>School of Natural Sciences and Mathematics, University of Texas at Dallas, Richardson, TX, USA, <sup>3</sup>Department of Earth and Environmental Sciences, Michigan State University, East Lansing, MI, USA, <sup>4</sup>Energy and Environment Directorate, Pacific Northwest National Laboratory, Seattle, WA, USA

### Key Points:

- The long-term effectiveness of pumping reduction-based groundwater conservation is dependent on lagged processes
- Vertical hydraulic conductivity ( $K_z$ ) controls if lagged responses are lateral-flow dominated or recharge-dominated
- Ignoring lagged processes overestimates aquifer lifetime by 32 and 133 years in lateral-flow and recharge-dominated settings, respectively

### Supporting Information:

Supporting Information may be found in the online version of this article.

### Correspondence to:

T. J. Glose and S. Zipper,  
[tomglose@ku.edu](mailto:tomglose@ku.edu);  
[samzipper@ku.edu](mailto:samzipper@ku.edu)

### Citation:

Glose, T. J., Zipper, S., Hyndman, D. W., Kendall, A. D., Deines, J. M., & Butler, J. J. Jr. (2022). Quantifying the impact of lagged hydrological responses on the effectiveness of groundwater conservation. *Water Resources Research*, 58, e2022WR032295. <https://doi.org/10.1029/2022WR032295>

Received 9 MAR 2022

Accepted 27 JUN 2022

**Abstract** Many irrigated agricultural areas seek to prolong the lifetime of their groundwater resources by reducing pumping. However, it is unclear how lagged responses, such as reduced groundwater recharge caused by more efficient irrigation, may impact the long-term effectiveness of conservation initiatives. Here, we use a variably saturated, simplified surrogate groundwater model to: (a) analyze aquifer responses to pumping reductions, (b) quantify time lags between reductions and groundwater level responses, and (c) identify the physical controls on lagged responses. We explore a range of plausible model parameters for an area of the High Plains aquifer (USA) where stakeholder-driven conservation has slowed groundwater depletion. We identify two types of lagged responses that reduce the long-term effectiveness of groundwater conservation, recharge-dominated and lateral-flow-dominated, with vertical hydraulic conductivity ( $K_z$ ) the major controlling variable. When high  $K_z$  allows percolation to reach the aquifer, more efficient irrigation reduces groundwater recharge. By contrast, when low  $K_z$  impedes vertical flow, short term changes in recharge are negligible, but pumping reductions alter the lateral flow between the groundwater conservation area and the surrounding regions (lateral-flow-dominated response). For the modeled area, we found that a pumping reduction of 30% resulted in median usable lifetime extensions of 20 or 25 years, depending on the dominant lagged response mechanism (recharge- vs. lateral-flow-dominated). These estimates are far shorter than estimates that do not account for lagged responses. Results indicate that conservation-based pumping reductions can extend aquifer lifetimes, but lagged responses can create a sizable difference between the initially perceived and actual long-term effectiveness.

## 1. Introduction

Irrigation uses the majority (69%) of fresh groundwater withdrawals in the United States (DeSimone et al., 2015; Dieter et al., 2018). In many aquifers supporting irrigated agriculture, heavy pumping has resulted in unsustainable water-level declines, threatening the economy and environment (Deines et al., 2020; Huggins et al., 2022; Scanlon et al., 2012). As groundwater is a limited resource, how to mitigate these declines to extend the usable lifetime of heavily stressed aquifers is a pressing question (Bierkens & Wada, 2019; Butler et al., 2020b; Castilla-Rho et al., 2019; Gleeson et al., 2020). In semi-arid environments with little access to surface water, groundwater conservation programs that seek to reduce pumping are one of the only viable options to decrease groundwater declines in the near to moderate term (Butler et al., 2020a; Deines et al., 2019; Hu et al., 2010).

The fundamental premise of groundwater conservation is to reduce outflows from the aquifer by reducing pumping. However, it is not clear how the effectiveness of such conservation initiatives might change in the future as the hydrological system in areas with groundwater conservation adjusts to the observed pumping reductions (Butler et al., 2020a; Deines et al., 2021; Foster et al., 2017). For example, the transit time for water at the land surface to percolate downward and become groundwater recharge can vary dramatically over the High Plains aquifer due to variations in unsaturated zone thickness and vertical hydraulic conductivity ( $K_z$ ), with estimates ranging from decades to centuries (Gurdak et al., 2008; Katz et al., 2016; McMahon et al., 2006; Zell & Sanford, 2020). Current management approaches are often implemented with a time horizon of years to decades (Miro & Famiglietti, 2019; Whittemore et al., 2018), while effective groundwater sustainability requires setting and meeting multi-generational goals (Gleeson et al., 2012). Evaluating groundwater conservation programs on

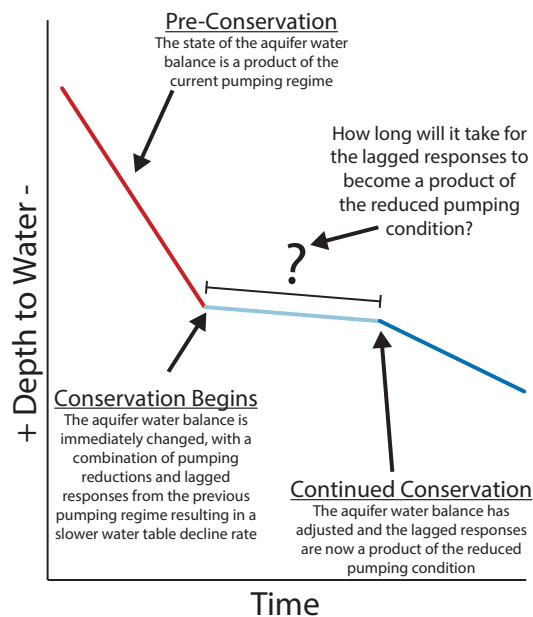


**Figure 1.** Graphical representation of hypothesized aquifer water balance changes due to pumping reductions. The initial reduction in pumping causes an immediate change to the aquifer water balance, resulting in an initial period of high effectiveness (light blue line) that wanes in time as lagged responses, such as groundwater recharge and lateral flow, adjust to the new pumping regime (dark blue line).

multi-generational timescales requires quantifying the long-term (decadal) response of aquifer water levels to pumping reductions.

The aquifer response to changes in pumping is a function of the pumping and a quantity termed net inflow, which is defined as total inflows (i.e., recharge, lateral inflows [LIs]) minus all non-pumping outflows (i.e., discharge to streams, vegetation, lateral outflows), and is mediated by hydrostratigraphic characteristics such as hydraulic conductivity and specific yield (Butler et al., 2016). However, the relative contributions of vertical and lateral flows to net inflow are poorly understood and difficult to parse (Butler et al., 2016, 2020a). While recent work has found that reductions in aquifer net inflow can decrease the effectiveness of groundwater conservation programs over time (Butler et al., 2020a), the mechanisms, timescales, and variations in magnitudes of lagged responses from different water balance components is not known. As a result, we do not know which lagged responses may impact overall groundwater sustainability, nor the timescales and controlling processes.

To address this knowledge gap, we seek to answer the question: *How do lagged responses to pumping reductions impact the effectiveness of groundwater conservation practices over time?* We hypothesize that when groundwater conservation initiatives, such as Kansas' LEMA program, are enacted, (a) the reduction in pumping causes an immediate change to the aquifer water balance, leading to a slowing of the water table decline rate (Figure 1, light blue line) and (b) over time, inflows will diminish because more efficient irrigation will lead to a reduction in deep percolation (water that drains below the rooting zone; Deines et al., 2021), which will eventually reduce recharge to the aquifer. Similarly, LI to the conservation area will diminish, as decreased pumping will reduce the hydraulic gradient driving water into the

area. In both situations, the result will be an increase in water table decline rates to an intermediate rate between the pre-conservation decline rate and the immediate post-conservation rate (dark blue line in Figure 1).

To test these hypotheses, we developed a variably saturated groundwater flow model for the Sheridan-6 Local Enhanced Management Area (SD-6 LEMA) based on historical observations and realistic conditions. To ensure that results were not reflective of site-specific phenomena, we employed a simplified surrogate modeling approach. We used this model to evaluate the long-term changes in the aquifer water balance associated with groundwater conservation, quantify the implications of lagged responses for estimates of usable aquifer lifetimes, and determine the physical controls on these lagged responses.

## 2. Methods

### 2.1. Study Region

We used the SD-6 LEMA in Kansas as a representative groundwater conservation program to evaluate these hypotheses. Located within the portion of the High Plains aquifer in northwestern Kansas, the SD-6 LEMA overlies a thick section of highly transmissive, unconsolidated sediments. There are no sources of surface water in the region and therefore groundwater is heavily pumped to support irrigated agriculture (Whittemore et al., 2018). LEMAs are a stakeholder-driven governance approach in which groundwater users (primarily irrigators) and groundwater management districts develop conservation plans. Once approved by the state, LEMAs are enforced by the state regulatory agency (Kansas Statutes Annotated 82a-1041, 2012). SD-6, the state's first LEMA, was initiated in 2013 in a 255-km<sup>2</sup> area in northwest Kansas with the stated goal of reducing annual pumping by 20% over a 5-year period (Figure 2, yellow outline). During that period, irrigators exceeded their goal, reducing pumping by 31% on average and slowing water table decline rates while maintaining similar economic returns (Deines et al., 2019, 2021; Golden, 2018; Whittemore et al., 2018). This initial success led to an extension of the SD-6 LEMA for an additional five years, the 2018 formation of a much larger LEMA that encompasses most of the northwest Kansas portion of the High Plains aquifer (Northwest Kansas Groundwater

Percent Change in Aquifer Thickness, Predevelopment to Average 2018-2020,  
Kansas High Plains Aquifer

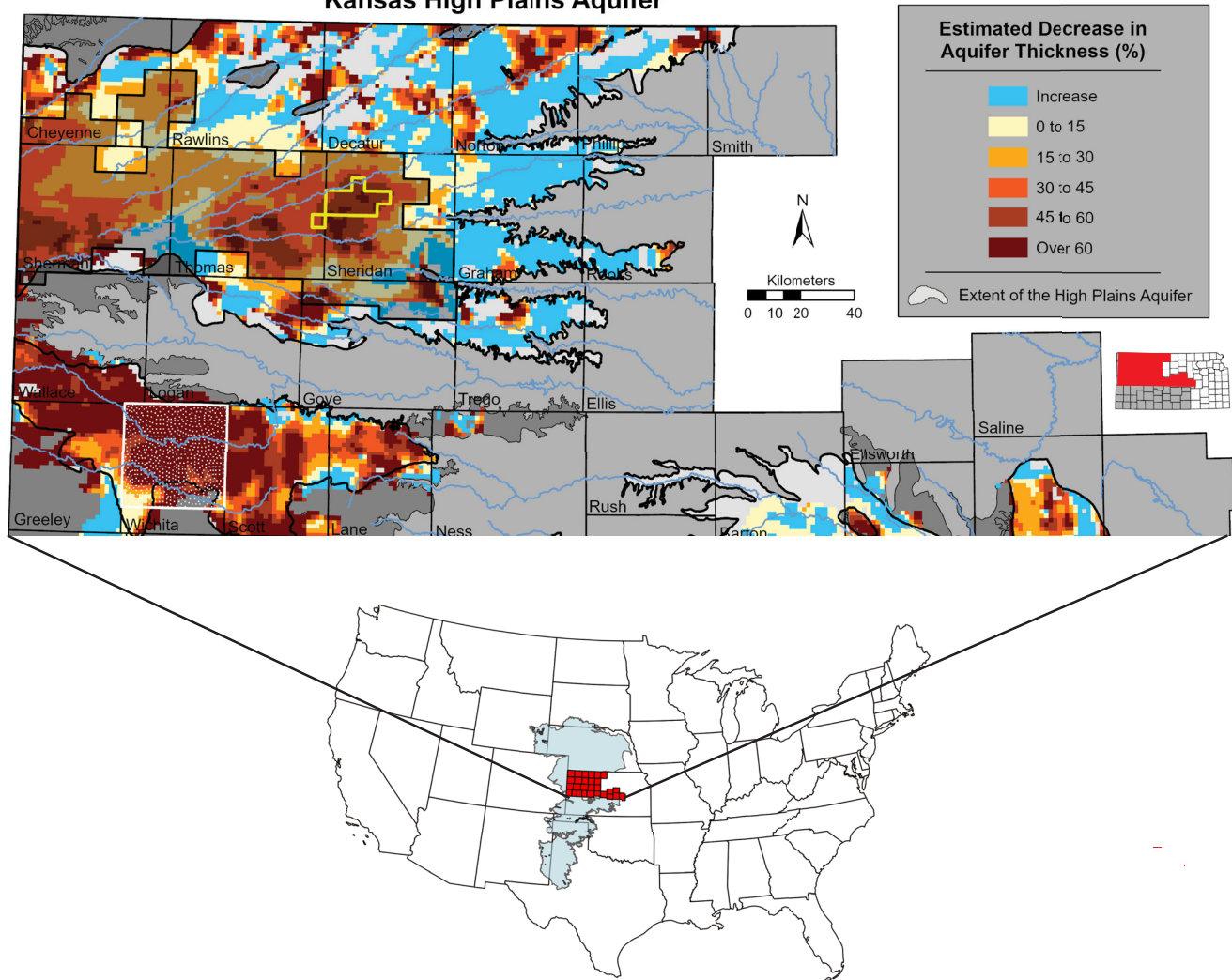


**Figure 2.** The large decrease in aquifer thickness from pre-development (~pre-1950) to present prompted the formation of the Sheridan-6 Local Enhanced Management Area (SD-6 LEMA) (yellow outline). Initial success of the SD-6 LEMA led to the formation of a LEMA for all of Northwest Kansas Groundwater Management District #4 (shaded area) and an additional LEMA in Wichita County (white stippled area).

Management District #4) (Figure 2, shaded area), and an additional 2021-initiated LEMA in west-central Kansas (Kansas Department of Agriculture, 2013, 2018, 2021) (Figure 2, white stippled area).

## 2.2. Model Overview

To test our hypotheses, we developed a variably saturated groundwater flow model of an arbitrary north-south linear transect that passes through the SD-6 LEMA (Figure 3). We elected to build a simplified model, rather than a fully-calibrated three-dimensional groundwater flow model, to better isolate the hydrological processes of interest, and more directly test our hypotheses by avoiding unnecessary site-specific complexity--an approach known as surrogate or archetypal modeling (Asher et al., 2015; Razavi et al., 2012; Voss, 2011a, 2011b; Zipper et al., 2018, 2019). Nevertheless, to ensure our model provided a reasonable simulation of the dominant processes in this region, we conducted an evaluation against field data from the SD-6 region, and conducted a sensitivity analysis to test the impact of simplifying assumptions on model results.

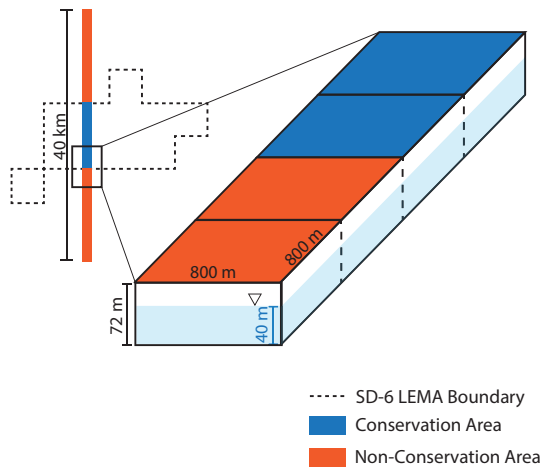


**Figure 3.** Conceptual diagram showing the location of the transect relative to the Sheridan-6 Local Enhanced Management Area (SD-6 LEMA), the two separate areas (conservation and non-conservation), the grid cell dimensions, the domain depth, and the starting head value representative of the pre-development period.

### 2.3. Model Construction and Input Data

We used the United States Geological Survey's MODFLOW-NWT program and constructed the model using the Python package FloPy (Bakker et al., 2016). The 40 km long domain consists of a single layer of 50 grid cells, each 800 m by 800 m in size, covering a total area of 32 km<sup>2</sup>. Each grid cell is roughly equivalent in area to a typical field size in the region (64.75 ha [160 acres]) and cell dimensions were set based on the typical distance between irrigation wells in the area to match spatial patterns of water withdrawals in the area (Figure S1 in Supporting Information S1). The model domain was split into two types of management practices (conservation and non-conservation; blue and orange areas, respectively, in Figure 3), which were represented in the model using different pumping and deep percolation rates as described below. The conservation area was made up of 14 grid cells while the non-conservation areas each consisted of 18 grid cells, with the four additional cells being added to remove the influence of edge effects from the northern and southern no-flow boundaries. The single model layer is 72 m thick and starting pressure heads were set to 40 m; these values represent the average depth to bedrock and pressure heads, respectively, of the area for the pre-development period (~pre-1950) (Fross et al., 2012). The top of the model is assumed to be below the rooting zone to remove the influence of evapotranspiration, overland flow, and discharge to surface water bodies.

Regional groundwater flow is perpendicular to our transect from west to east (Fross et al., 2012, Figure S2 in Supporting Information S1), so we included a lateral flow boundary condition on the west side and a no-flow boundary on the east to represent the net lateral flow entering the modeled area, which is distinct from the vertical inflow from groundwater recharge. Since our model is a north-south transect, this approach reduces the number of uncertain parameters by lumping inflow from the west and outflow to the east into a single net LI term. We varied net lateral flows along with the model hydrostratigraphic properties as described in Section 2.4.

Pumping and deep percolation rate time series were developed using a combination of historical annual precipitation depth, regression model-based historical pumping data (1955–1992) (Wilson et al., 2021), and measured pumping volumes (1993–2018). We estimated annual pumping volumes by establishing relationships between annual areally averaged precipitation depth and applied irrigation depth during the 2000–2018 period, the period after a large majority of irrigators had transitioned from traditional high pressure center pivot irrigation to more efficient center pivot with drop nozzle irrigation (Figure 4a) (Pfeiffer & Lin, 2010; Rogers & Lamm, 2012).

We first estimated annual areally averaged applied irrigation depth as the total pumping volume from wells within SD-6 divided by the total area. Observed pumping rates from the SD-6 LEMA were modified to account for the climate-adjusted 27% reduction in pumped volume observed during the first 4 years of the LEMA using the approach of Whittemore et al. (2018) and Butler et al. (2020a). We then developed a relationship between precipitation and irrigation depth for the “No Conservation” portions of the domain that included the period after the establishment of the SD-6 LEMA (2000–2018). We developed two additional relationships to simulate conservation practices by modifying the “No Conservation” relationship (Figure 4a): (a) a 20% pumping reduction scenario based on the legal requirements for the SD-6 LEMA; and (b) a 30% pumping reduction scenario that more closely reflects observed irrigator behavior.

For each pumping scenario, we then calculated the applied pumping volume for each grid cell as the product of irrigation depth from the statistical relationship (Figure 4a) and the area of the grid cell. We disaggregated the estimated annual pumping volume uniformly over a 103-day period, which was the average time between the onset and cessation of irrigation pumping in the region interpreted from high temporal-resolution well observations (Butler et al., 2019). Pumping was simulated using MODFLOW's well (WEL) package. As discussed in Section 2.2, our surrogate modeling approach was not intended to precisely represent observed spatial pumping dynamics within the SD-6 LEMA, but rather the average aquifer response to typical regional pumping. To reflect that the estimated pumping volume is representative of the entire SD-6 area, which is heavily irrigated, we placed a pumping well in each individual grid cell both inside and outside the conservation area. Due to the small

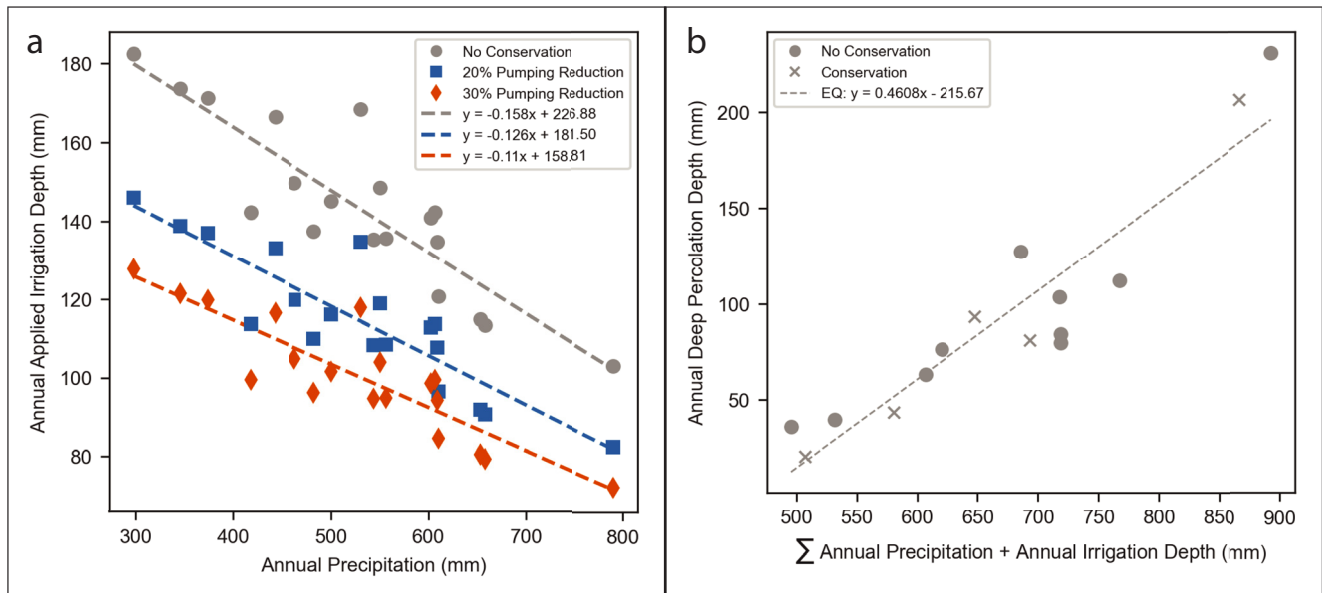


**Figure 4.** Annual statistical relationships for: (a) applied irrigation depth and (b) deep percolation depth.

amount of north-south variation in precipitation in our study domain (Figure S3 in Supporting Information S1), we used the same precipitation for estimating pumping in all grid cells so pumping was initially uniform within the conservation and non-conservation areas.

The model simulated flow through variably saturated porous media using the unsaturated zone flow (UZF) package, which uses a kinematic-wave approximation to solve the 1-D Richard's equation (Niswonger et al., 2006; Smith, 1983; Smith & Hebbert, 1983). While numerous models can simulate variably saturated flow, the UZF package for MODFLOW has several advantages for our purposes, including documented applications in thick vadose zones (Hunt et al., 2008; Nazarieh et al., 2018), computational efficiency (Kennedy et al., 2016; Niswonger & Prudic, 2009), and widespread use (Bailey et al., 2013; Hou et al., 2020; Morway et al., 2013). Since the top of our model domain represents the bottom of the root zone, we provided UZF with annual values of deep percolation from a linear model fit between simulated deep percolation from a calibrated crop model for the SD-6 area with and without conservation (Deines et al., 2021), and the sum of annual precipitation and applied irrigation depth following Scanlon et al. (2006) (Figure 4b). Like pumping, annual deep percolation values were uniformly disaggregated to daily values over the 103-day pumping period, since water inputs to the soil column (both precipitation and irrigation) are primarily concentrated during the growing season. The SALUS model that generated the deep percolation estimates simulates the root zone water balance including precipitation, evaporation, root water uptake, and irrigation, with irrigation being the dominant driver of deep percolation rates during the pumping season (Deines et al., 2021). Unlike the separate relationships required for pumping under each conservation scenario, only one relationship is needed to estimate deep percolation because the effects of groundwater conservation are accounted for in the annual irrigation depth term. These relationships (Figures 4a and 4b) were used to generate deep percolation rate time series for both the evaluation and projection periods as well as pumping rate time series for the projection period (Figure 5). Pumping rate time series for the evaluation period were generated using a combination of regression model-based and measured pumping rates.

Our simulations spanned 201 years (1900–2100), which can be divided into three periods: spin-up (1900–1954), historical (1955–2019), and projection (2020–2100). The 55-year spin-up period is prior to the onset of high capacity pumping in the region so the only fluxes in/out of the domain are deep percolation, which was applied at a rate of  $5 \times 10^{-4} \text{ m d}^{-1}$  ( $51.5 \text{ mm yr}^{-1}$ ) to approximate pre-development recharge in the area (Fross et al., 2012; Hansen, 1991), and the applied LIs. To ensure that recharge and LI did not change the prescribed pre-development saturated zone pressure heads, a drain was placed at the pre-development water level (40 m) across the domain. This approximates the effect of the regional streams that drained the system during the pre-development period. After the spin up period, a mix of regression-estimated (1955–1992) (Wilson et al., 2021) and measured pumping

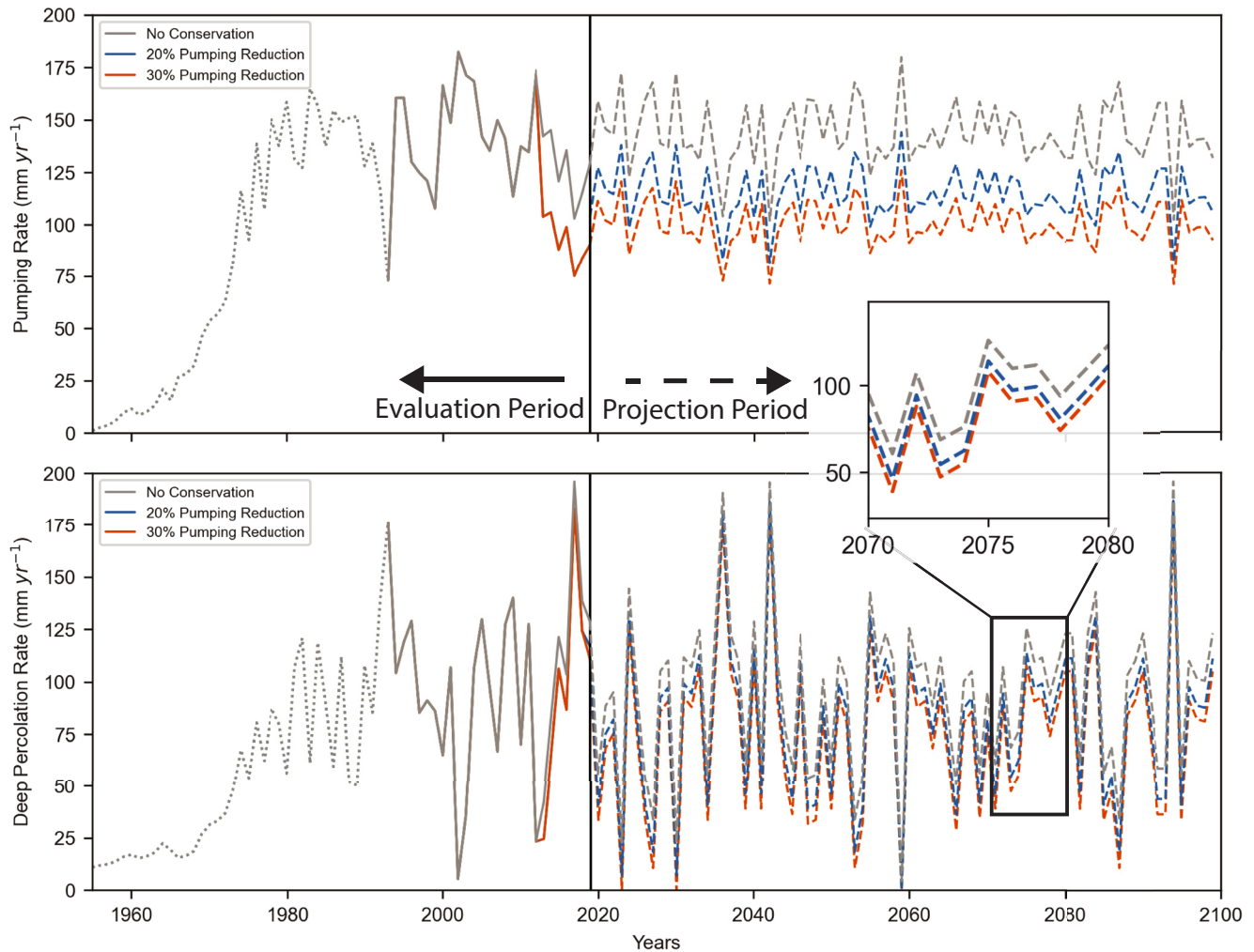


**Figure 5.** Pumping (upper) and deep percolation (lower) rates calculated from the statistical relationships in Figure 4. For the three very dry years in the prediction period, the statistical relationship in Figure 4b produced negative deep percolation rates; these years were assigned a rate of 0 m d<sup>-1</sup>. For the historical period, pumping rate and deep percolation are shown only for the 30% pumping reduction scenario (orange) as this best represents observed irrigator behavior.

volumes (1993–2018) for the SD-6 area was used to define pumping rate inputs for the model (Figure 5). Pumping data for the year 2019 was estimated using the statistical regression as pumping data were not available, but this year was included in the evaluation period as water level change and head data were available at the time of model development. As observed irrigator behavior within the LEMA was close to the 30% pumping reduction scenario, we used the 30% reduction pumping rates for 2013–2019. The projection period (2020–2100) allows us to evaluate the long-term implications of pumping with the baseline and the two reduction (20% and 30%) pumping scenarios. For the projection period, we randomly sampled annual precipitation from the historical precipitation record to estimate pumping and deep percolation for each year based on the relationships shown in Figure 4 since there are no consistent long-term historical (Lin et al., 2017) or projected (Figure S4 in Supporting Information S1) precipitation trends in this region, and historical precipitation patterns do not exhibit significant temporal autocorrelation (Butler et al., 2020a).

#### 2.4. Model Evaluation and Evaluation of Control Parameters

We used a Latin hypercube sampling scheme (McKay et al., 1979) to identify the model parameters that best reproduced observed hydrological data, and evaluate the sensitivity of model output to each parameter and the interactions between parameters (Zipper et al., 2018). Our Latin hypercube sample consisted of 2,000 near-random, unique sets of hydrostratigraphic parameters (vertical saturated hydraulic conductivity,  $K_z$ ; specific yield,  $S_y$ ;

**Table 1**  
*Parameter Space Ranges for the Latin Hypercube Sampling Scheme*

Parameter	Lower bound	Upper bound
$\log_{10}$ vertical hydraulic conductivity ( $\text{m d}^{-1}$ ) <sup>a</sup>	−6	1
Specific yield (−) <sup>b</sup>	0.06	0.18
Brooks and Corey Epsilon (−) <sup>c</sup>	2	5
$\log_{10}$ lateral inflows ( $\text{m d}^{-1}$ ) <sup>b</sup>	−6	−3

*Note.* As we are taking a surrogate modeling approach, ranges were extended outside of their observed values for the area to allow the parameter space to be fully explored.

<sup>a</sup>(Fross et al., 2012). <sup>b</sup>(Butler et al., 2016). <sup>c</sup>(Brooks & Corey, 1966).

Brooks and Corey epsilon,  $\epsilon$ ) and LI, which were selected from a uniform distribution over the parameter space shown in Table 1. We ran one simulation using each parameter set to explore lagged responses to groundwater conservation across a range of hydrogeological settings and to reduce the risk of identifying a local optimum as the best parameter set.

Horizontal hydraulic conductivity and saturated water content were held constant at  $20 \text{ m d}^{-1}$  and 0.25, respectively, to reflect average values in the SD-6 LEMA area (Fross et al., 2012). The UZF package relies on the Brooks and Corey function to calculate unsaturated  $K_z$  (Brooks & Corey, 1966). This function requires residual water content, here approximated for each parameter set by taking the  $S_y$  value for each set and subtracting it from the saturated water content (Niswonger et al., 2006). A value of 0.005 was added to the calculated residual water content to ensure that the unsaturated hydraulic conductivity value did not start at a value of zero.

We evaluated the performance of each of the 2,000 simulations via comparison to the observed groundwater level data for the 1999–2019 period, which represents the longest continuous record of reliable observations within the SD-6 LEMA (KGS WIZARD Database; <http://www.kgs.ku.edu/Magellan/WaterLevels/index.html>). The goal of this study is to ensure that the dominant processes (e.g., pumping reductions and lagged responses) are appropriately simulated while not overparameterizing the model since our focus is not on site-specific heterogeneity (Konikow & Bredehoeft, 1992).

We quantified model performance for each parameter set using a two-step approach. First, as the area has experienced significant drawdown, we eliminated model runs in which the head in the model domain at the end of the historical period (2019) was still at or above pre-development levels (Fross et al., 2012). For the remaining runs, we calculated the Kling-Gupta Efficiency (KGE; Kling et al., 2012) score for both the annual water table elevation and the interannual change in water table elevation, which are based on measurements taken each January in the LEMA area. We selected these two metrics to ensure that both the long-term and interannual dynamics were simulated reasonably, and used the minimum (lower-performing) of these two KGE values as the final KGE score for that parameter set. We then divided the model runs into four performance groups: poor ( $\text{KGE} < -0.41$ , which indicates that the model results are worse than the mean of the observations; Knoben et al., 2019), low ( $-0.41 < \text{KGE} < 0$ ), medium ( $0 < \text{KGE} < 0.5$ ), and high ( $\text{KGE} > 0.5$ ). A KGE score of 1 would indicate a perfect match between a simulation and observations. Only runs in the high performance group were analyzed for the projection period because those parameter sets were able to reasonably approximate historical hydrological conditions. We also conducted a sensitivity analysis to determine the influence of several simplifying assumptions (model discretization, model homogeneity, uniform distribution of pumping wells) on model results. To do this, we ran five additional model scenarios with a smaller grid cell dimension in which each simplification was analyzed further (see Text S1, Figure S5, and Table S1 in Supporting Information S1 for more details).

The models selected for projection were run to the year 2100 and the extension of the usable aquifer lifetime was quantified for the 20% and 30% pumping reduction scenarios. For each parameter combination and pumping scenario, the extension of the usable aquifer lifetime is calculated as the number of years that water levels in the aquifer remain above a minimum threshold relative to the baseline “No Conservation” scenario. For this region, we assumed that a minimum saturated thickness of 8 m is required for large-scale irrigation to allow for sufficient transmissivity, and therefore well yield, along with pumping-induced drawdown in the well (Butler et al., 2020a; Deines et al., 2020).

### 3. Results and Discussion

#### 3.1. Recharge and Lateral-Flow-Dominated Inflows

We found that many parameter combinations were able to reproduce the historical head and head change observations (Figure 6). Of the 2,000 parameter combinations tested, there were 122 simulations rated as high performance (Figure 6, dark red circles,  $\text{KGE} > 0.5$ ). An additional 214 were rated as medium, 126 as low, 1,090 as poor, and 448 were discarded due to no simulated drawdown (Figure 6). Within parameter pairs, there are several clusters that occur throughout the parameter space (Figure 6b), the most evident occurring between LI

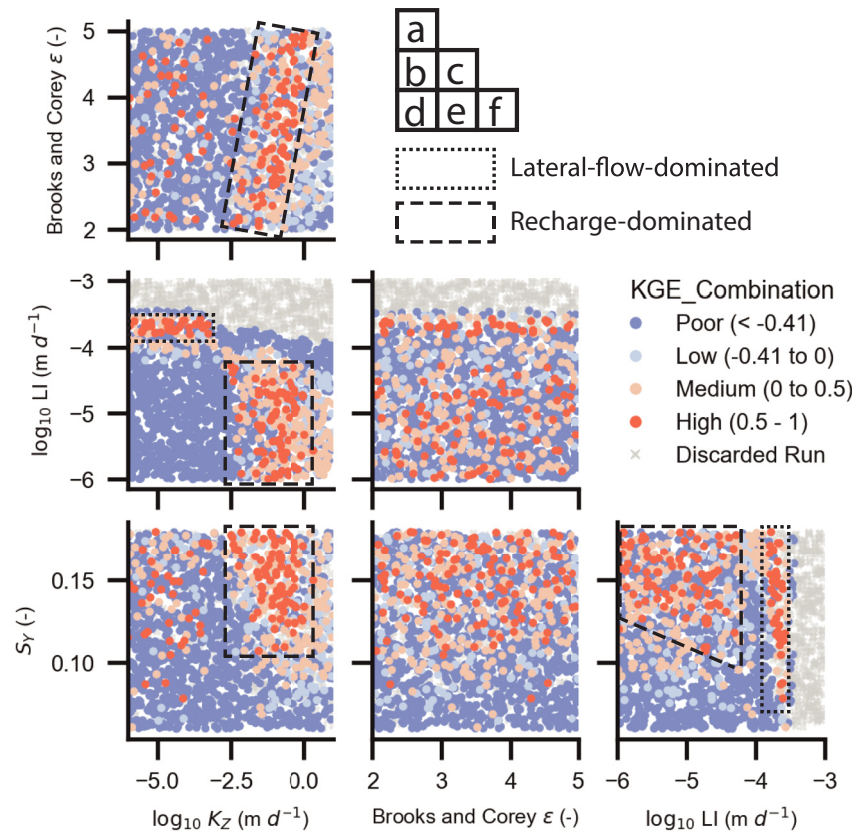


**Figure 6.** Model fit for each pairwise combination of parameters for the 30% pumping reduction scenario. Each point shows one simulation, colored by the Kling-Gupta Efficiency (KGE) score for the model evaluation period. The dotted and dashed inset rectangles indicate grouping clusters for the lateral-flow- and recharge-dominated cases.

and vertical hydraulic conductivity ( $K_z$ ). In parameter space, these two clusters correspond to a high LI/low  $K_z$  zone, in which lateral groundwater flow is the dominant inflow to the aquifer, and a low LI/high  $K_z$  zone, in which vertical groundwater recharge is the dominant inflow to the aquifer. Since each plot represents the combination of two variables, subplots with intermingled high and low performing model runs (i.e., Figures 6c and 6e) indicate that those variables have a relatively low influence on simulated groundwater response to pumping and conservation and that model performance is primarily controlled by other variables. In contrast, variable combinations that have a strong influence on simulated results (i.e., Figure 6b) show a clearer separation of high and low performing model runs.

For the lateral-flow-dominated case, the parameter sets that yield high KGE scores have LI values between  $1.6 \times 10^{-4}$  and  $2.5 \times 10^{-4}$  m d<sup>-1</sup> and  $K_z$  values between  $1 \times 10^{-6}$  (the lower bound of the parameter space tested) and  $5 \times 10^{-4}$  m d<sup>-1</sup>. However, for the Brooks and Corey  $\epsilon$  and  $S_y$  there are no clear thresholds, indicating that the rate of lateral flow is the controlling factor. The ranges of  $K_z$  and LI values with good fits in the recharge-dominated case are opposite of the lateral-flow-dominated case, with higher  $K_z$  values (from  $3.5 \times 10^{-3}$  to  $1$  m d<sup>-1</sup>) and lower LI values (from  $5 \times 10^{-5}$  m d<sup>-1</sup> to the lower bound of the parameter space tested,  $1 \times 10^{-6}$  m d<sup>-1</sup>) (Figure 6b). In contrast to the lateral-flow-dominated case, the recharge-dominated case is also sensitive to the Brooks and Corey  $\epsilon$  and  $S_y$ . As  $K_z$  approaches  $1$  m d<sup>-1</sup>, the value of  $\epsilon$  steadily increases from 2 to 5 (Figure 6a). The range of  $S_y$  is also limited based on  $K_z$ , with  $S_y$  values between 0.1 and 0.18 necessary to generate KGE scores of  $\geq 0.5$  (Figure 6d). Vertical hydraulic conductivity is not the only controlling factor in the recharge-dominated case. As the value of LI increases toward its upper limit of  $5 \times 10^{-5}$  m d<sup>-1</sup>, the range of  $S_y$  also expands with its lower limit dropping from 0.13 to 0.1 (Figure 6f). The interplay between hydrostratigraphic parameters plays a more prominent role in the recharge-dominated scenario. Along with  $K_z$ , the Brooks and Corey  $\epsilon$  and  $S_y$  influence the rate and volume of vertical water movement through the thick vadose zone, respectively, and therefore influence the performance of the model.

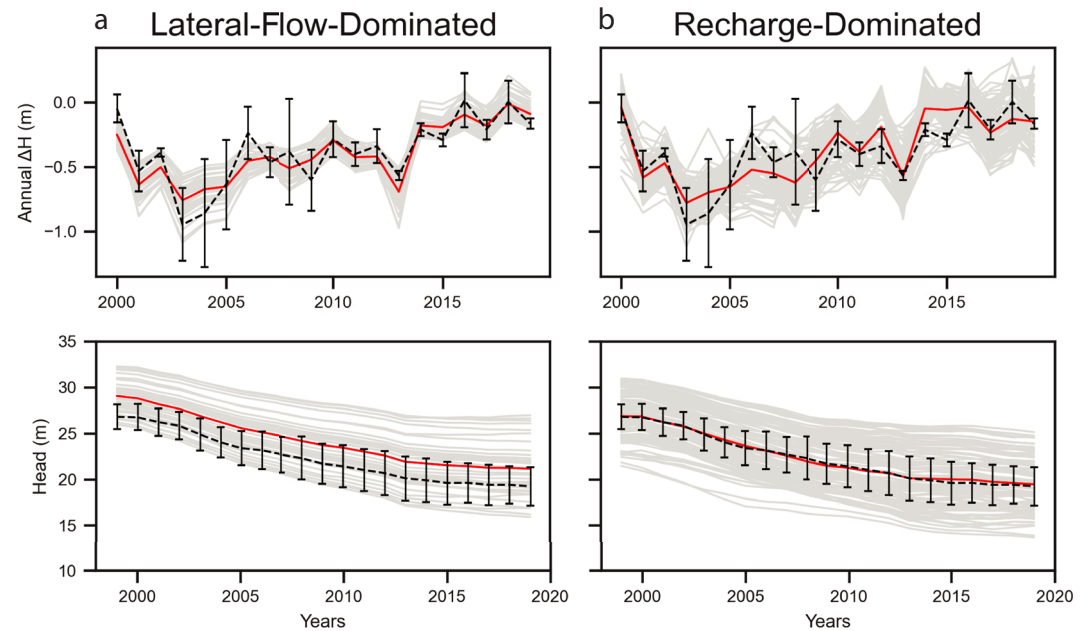


**Figure 7.** Results for the 30% pumping reduction scenario of observed (black, dashed line), simulated (light gray, solid lines), and average simulated (red lines) interannual change in pressure head and annual pressure head values for the (a) lateral-flow-dominated and (b) recharge-dominated cases. Simulation results presented for the center cell in the conservation area, the error bars show one standard deviation about the mean of the observed data.

For both the lateral-flow-dominated and recharge-dominated cases, the average simulated interannual change in pressure head and annual pressure head values (Figures 7a and 7b, red lines) reasonably align to the average observed values (Figures 7a and 7b, dashed lines), indicating that the model is reasonably capturing the annual and interannual dynamics of the natural system. While the recharge-dominated simulations are closer to the mean of the observed head values, lateral-flow-dominated simulations were generally within one standard deviation of the mean of all observations and better matched observed interannual head change. The average KGE score and root mean square error (RMSE) were quantified for all high-performing lateral-flow- and recharge-dominated runs. In the lateral-flow-dominated cases the KGE score and RMSE for the interannual change in head are 0.687 and 0.142 m, respectively. For the annual head, these values are 0.776 and 2.226 m, respectively. In the recharge-dominated cases the KGE score and RMSE for the interannual change in head are 0.644 and 0.205 m, respectively. For the annual head, these values are 0.763 and 2.507 m, respectively. We also tested the sensitivity of our model results to several of the simplifying assumptions adopted in our surrogate modeling approach: model discretization, model homogeneity, uniform distribution of pumping wells. We found that increasing the complexity of our model did not substantially affect our results or interpretations (Text S1, Figure S5, and Table S1 in Supporting Information S1).

The wide variety of parameters that lead to reasonable agreement with the observed data indicates that multiple interpretations of the underlying processes that dictate groundwater recharge in areas with thick vadose zones are equally valid, following the principle of equifinality (Beven, 2006). In groundwater modeling, parameter estimation often seeks to find a local or global optimum to match limited observations while minimizing an objective function using software such as PEST (Doherty, 2015) or UCODE (Poeter & Hill, 1999). However, the hunt for an ideal parameter set that results in simulated values closely matching observed values can ignore other possible parameter sets that perform nearly equally well (Liu et al., 2022; Savenije, 2001). This is true for our surrogate model of the SD-6 area as the lack of vadose zone observation data paired with an exploration of a wide parameter space resulted in two possible and equally valid mechanisms, or combination of mechanisms, that affect the long term performance of pumping reduction-based groundwater conservation initiatives. In practice, these two end members define a spectrum and the actual setting is found somewhere on this spectrum. Since the long-term response of an aquifer to pumping and conservation will be dictated by the relative magnitude of each of these processes, this further highlights the need to better understand when each of these lagged processes is dominant.

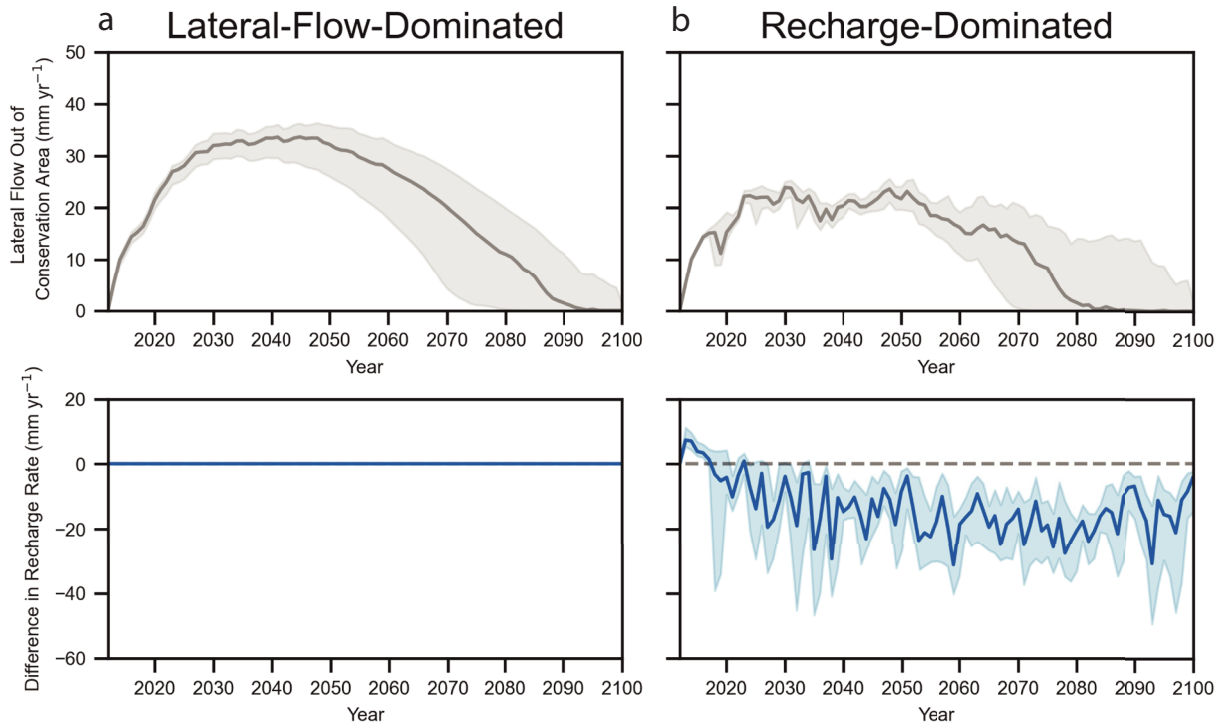


**Figure 8.** Average time series of simulated lateral outflow from the conservation area to the non-conservation area (gray lines, upper plots) and difference in recharge rate between the conservation area and the non-conservation area (blue lines, lower plots) for (a) the lateral-flow-dominated and (b) recharge-dominated cases. Thick lines represent average values across all model runs used for the projections and the shading indicates the interquartile range.

### 3.2. Lagged Responses to Conservation in Recharge- and Lateral-Flow-Dominated Conditions

Recharge-dominated and lateral-flow-dominated cases exhibit different long-term hydrological responses to groundwater conservation due to differences in lagged changes to the aquifer water balance. In lateral-flow-dominated settings, changes in deep percolation caused by pumping reductions do not significantly impact recharge rates within the 80-year projection period because recharge rates are low to begin with and changes in deep percolation take a long time to propagate down to the water table (Figure 8a). Following reductions in pumping, water table decline rates undergo an initial dramatic reduction then increase through time before stabilizing at an intermediate rate, consistent with our hypothesis (Figure 1). The increase occurs because the initial reduction within the conservation area creates a lateral hydraulic gradient that drives lateral flow into the surrounding non-conservation area; this phenomenon is further discussed in Section 3.3. In the lateral-flow-dominated case, high fluxes of net LI compensate for the lack of recharge. This case only applies when  $K_z$  values are low as any increase in recharge would add too much water to the aquifer, resulting in unrealistic rises in the water table. When LI is the controlling mechanism, the Brooks and Corey  $\epsilon$  has a negligible impact on the effectiveness of the pumping reductions.

In recharge-dominated cases, deep percolation can travel through the unsaturated zone rapidly enough that changes in applied irrigation water can alter the rate of groundwater recharge within our simulation period. Reductions in pumping decrease the amount of water that is applied in excess of crop water demands, and thus reduce the rate of deep percolation (Figure 4b). Unlike the lateral-flow-dominated case where there is no difference in recharge between the conservation and non-conservation areas over the time span of this analysis, the effects of changing deep percolation led to a reduction in groundwater recharge within the conservation area relative to the non-conservation area (Figure 8b). Once recharge decreases in response to the reduced pumping condition, water table decline rates increase, consistent with our hypothesis (Figure 1). However, even in recharge-dominated settings, conservation can lead to substantial changes in transect-parallel lateral outflows. These lateral outflows across the border of the conservation area reach up to  $\sim 25 \text{ mm yr}^{-1}$ , which is comparable to the difference in recharge between the conservation and non-conservation areas (Figure 8b).

Lateral flow and recharge have distinct time lags from the onset of groundwater conservation measures. For the lateral-flow-dominated cases, flow out of the conservation area begins with the start of pumping reductions and increases quickly with the development of a head gradient between the conservation and non-conservation areas. Eventually, lateral outflow peaks at a rate of  $\sim 34 \text{ mm yr}^{-1}$  from 2030 to 2050, or  $\sim 17$  to  $\sim 37$  years after the onset of conservation (Figure 8a). After 2050, lateral outflow gradually decreases due to a decline in the head gradient between the conservation and non-conservation areas, typically reaching  $0 \text{ mm yr}^{-1}$  between 2080 and 2100 depending on the case. In the recharge-dominated cases (Figure 8b), lateral flow out of the conservation area follows a similar pattern, though with a lower peak ( $\sim 24 \text{ mm yr}^{-1}$ ) and more interannual variability. The interannual variability in lateral outflows in the recharge-dominated cases is due to differences in recharge rates between the conservation and non-conservation areas, with larger lateral outflows when the recharge differences between the conservation and non-conservation areas are greater because this induces a larger hydraulic gradient between the two areas. For the recharge-dominated cases, there is an immediate short lived-period of positive differences in recharge rates, with recharge into the conservation area greater than into the non-conservation area because the reduction in water table decline rates allows more recharge to reach the water table than at higher decline rates. After 5 years, recharge rates in the groundwater conservation area adjust to the lower deep percolation rates associated with the reduced pumping condition, resulting in a negative difference for the rest of the simulation.

These differences between the lateral- and recharge-dominated cases indicate that, in settings with higher values of  $K_z$  (in our case,  $>0.0035 \text{ m d}^{-1}$ ; Figure 6), excess applied irrigation water can traverse the thick vadose zone that is present in western Kansas and ultimately recharge the water table. However, vertical hydraulic conductivity is not the only controlling factor in the recharge-dominated cases, as LI,  $S_y$ , and Brooks and Corey  $\epsilon$  also play important roles in the long-term effectiveness (see Figure 6). In cases where  $S_y$  is low, high-performing parameter sets tend to have a greater LI to compensate for the low drainable pore space. When  $K_z$  values are low, Brooks and Corey  $\epsilon$  values must be low as well to allow for the calculated unsaturated hydraulic conductivity value to be high enough to transmit water through the vadose zone at a rapid enough rate to initiate groundwater recharge. As  $K_z$  increases, so must the Brooks and Corey  $\epsilon$ , limiting the value of unsaturated hydraulic conductivity and preventing the aquifer from becoming inundated with excess water.

### 3.3. Effects of Lagged Responses on Aquifer Usable Lifetime

These lagged responses to groundwater conservation led to different estimates of the degree to which conservation extends the usable aquifer lifetime. The lateral-flow-dominated cases had an average extension of 15 years for a 20% pumping reduction and an average extension of 25 years for a 30% reduction (Figures 9a and 9c). Results were similar for the recharge-dominated cases, where the average extension was 12 years with a reduction in pumping of 20% and 20 years for a pumping reduction of 30% (Figures 9b and 9d). Using the start of the initial SD-6 LEMA in 2013, the remaining usable lifetime can be quantified. For the recharge-dominated cases, if no pumping reductions are applied, the water table will fall below 8 m of saturated thickness (the minimum thickness capable of supporting irrigated agriculture; Butler et al., 2020a) in 2047. If pumping is reduced by 20% or 30%, the aquifer lifetime will be extended to 2059 and 2067, respectively. For the lateral-flow-dominated cases, the water table will fall below eight m of saturated thickness in 2045 in the absence of pumping reductions. With a 20% and 30% pumping reduction, the lifetime is extended to 2060 and 2070, respectively. The numbers found in this study are within the envelope found by Butler et al. (2020a) who used a water balance approach to quantify the extension of usable lifetime under various exploratory scenarios, but does not differentiate between lagged changes in recharge and lateral flow. Our analysis extends this previous work by quantifying the relative importance of these two drivers of long-term change in net inflows.

In general, these results indicate that the effectiveness of groundwater conservation could be overestimated if only using data from the period between initiation of pumping reductions and the onset of the lagged responses. Using the observed heads from 2013 to 2019 and extrapolating until the aquifer thickness drops below 8 m, the usable lifetime extends to 2107 (Figures 9a and 9b, black dashed line). For the lateral-flow-dominated cases, this value drops to 2098 for the 20% pumping reduction scenario and 2102 for the 30% pumping reduction scenario (Figure 9a, blue and orange dashed lines). The recharge-dominated cases result in a much greater duration with the usable lifetime extending to 2142 for the 20% pumping reduction case and 2220 for the 30% pumping reduction case (Figure 9b, blue and orange dashed lines). Ignoring the impacts of lagged responses by extrapolating the

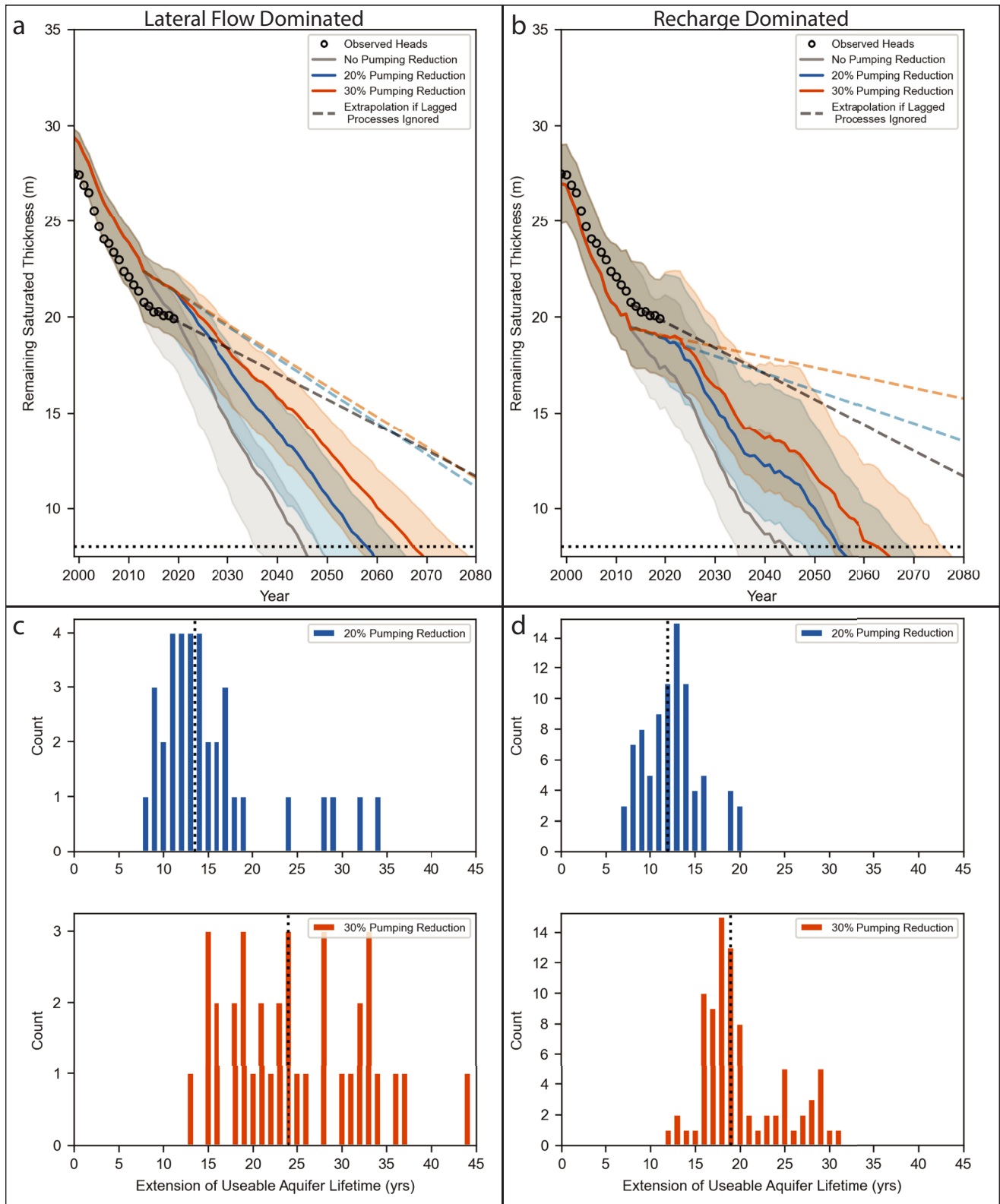
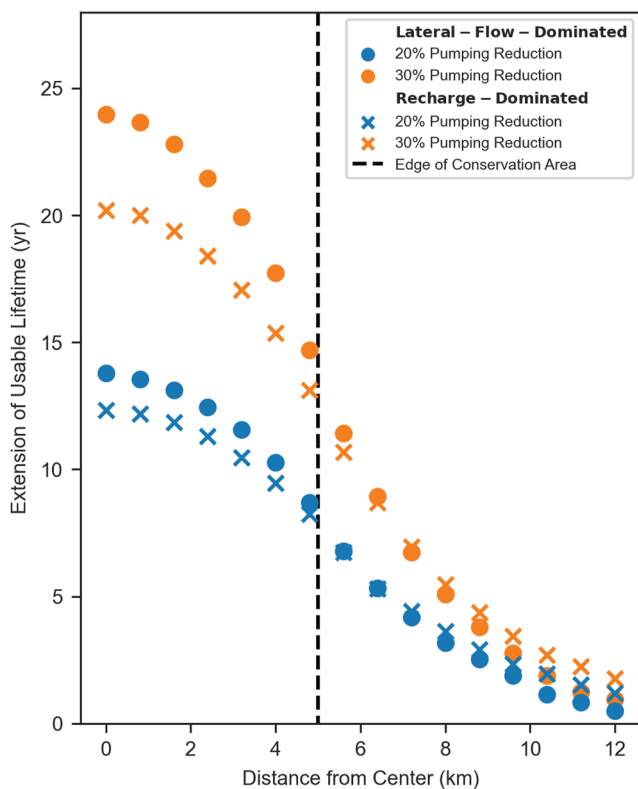


Figure 9.



**Figure 10.** Average extension of usable aquifer lifetime for the lateral-flow-dominated (circles) and recharge-dominated (Xs) scenarios compared to distance from the center of the conservation area. Extension of usable aquifer lifetime was quantified for the center of each grid cell by calculating the difference in time between when the “No Conservation” scenario and the 20% and 30% pumping reduction scenarios reached eight m of saturated thickness, which is the minimum saturated thickness capable of supporting large-scale pumping.

initial aquifer response to pumping reductions results in a dramatic overestimate of the effectiveness of these conservation methods. The subsequent increase in the water table decline rate dictates the long term effectiveness of groundwater conservation strategies. Understanding the mechanisms that control these lagged responses can manage stakeholder expectations and lead to the design of more effective conservation strategies that can further extend the usable lifetime of stressed aquifers. For example, as the effectiveness of initial conservation measures wanes and a return to increased water table decline rates begin to be observed, Butler et al. (2020a) have shown that additional pumping reductions can further extend usable aquifer lifetimes.

### 3.4. Implications for Isolated Conservation Areas Within Heavily Stressed Regional Aquifers

Conservation strategies are most urgently needed in heavily stressed aquifers. Since changes to groundwater flow can transmit the impacts of land use decisions to neighboring parts of the landscape (Zipper et al., 2017), it is important to understand how impacts of pumping reductions could extend beyond the borders of the conservation area. We found that changes in transect-parallel lateral flow caused by conservation can subsidize those outside the conservation area by slowing the rate of aquifer decline in the non-conservation area (Figure 10). As our modeling setup is symmetric, the largest extension of usable lifetime occurs in the center of the conservation area (values plotted in Figure 9) and decreases toward and across the boundary between the conservation and non-conservation areas. These cross-boundary effects are greatest under the transect-perpendicular lateral-flow-dominated cases but also occur in recharge-dominated cases due to the transect-parallel lateral hydraulic gradient changes discussed above. Without any reductions in pumping outside the conservation area, the non-conservation area gains at least 5 years of additional usable aquifer lifetime at distances of approximately 2 km from the boundary for the 20% pumping reduction case and between 3.5 and 4 km for the 30% pumping reduction case. Extensions of the usable aquifer lifetime at 7 km from the boundary range between about 0.75 and 2 years. Effectively, the gains in usable aquifer lifetime brought about by conservation can spill

out of the conservation area, indicating that the benefits of pumping reductions may extend beyond the borders of conservation areas by subsidizing their neighbors. However, the magnitude of this effect is likely dependent on the horizontal conductivity value and the size and shape of the conservation area. We would anticipate a smaller transect-parallel lateral flow subsidy in areas with a lower horizontal hydraulic conductivity and/or a smaller perimeter-to-area ratio relative to the conditions simulated here, which would result in a longer extension of usable aquifer lifetime in the conservation area.

While our surrogate model simulations found net outflow across the LEMA boundary, in practice many over-exploited areas where groundwater conservation measures may be implemented are closed basins and therefore this may manifest through other impacts such as a reduction in cross-boundary inflows to the conservation area (Pauloo et al., 2021). In either case, this indicates that the benefits of pumping reductions can extend beyond the boundaries of the areas with groundwater conservation initiatives, with potential socio-political impacts. Since heavily-pumped areas may preferentially exist in high productive aquifers with high transmissivity, the lateral cross-boundary effects we identify here are likely possible in many stressed aquifers. For instance, if pumping reductions are implemented in trans-boundary aquifers, lagged responses should be accounted for to ensure that

**Figure 9.** (a and b) Median simulated saturated thickness for the three pumping scenarios for (a) lateral-flow-dominated and (b) recharge-dominated cases. Dashed lines represent extrapolated remaining saturated thickness if the impact of lagged responses is ignored. The horizontal dotted line represents the minimum saturated thickness (8 m) needed for large-scale irrigated agriculture. (c and d): Median extension of usable lifetime (vertical black dotted line) and histogram of number of occurrences for the 20% and 30% pumping reduction scenarios for (c) lateral-flow-dominated and (d) recharge-dominated cases. Shaded areas in panels (a and b) represent the interquartile range of the simulated projections.

water resources are shared equitably (Callegary et al., 2018; Lee et al., 2018; Lipponen & Chilton, 2018; Sindico et al., 2018).

### 3.5. Limitations and Future Research Needs

Although the modeling framework presented here reproduced the interannual and annual dynamics of the observed natural system (Figure 7), there are several limitations to our approach that may affect the results. First, aquifers are inherently complex, spatially heterogeneous, and frequently lack sufficient observation data. Our analysis deliberately simplified this complexity into a homogeneous surrogate model in order to isolate the role of lagged hydrological responses in areas of groundwater conservation, and therefore does not capture the intricacies of the natural world, such as spatial changes in depth to bedrock, strata discontinuity, incorporation of regional groundwater gradients, or heterogeneous distributions of pumping wells. However, our sensitivity analysis demonstrated that our conclusions were robust to these simplifications (see Text S1, Figure S5, and Table S1 in Supporting Information S1 for details). Because our surrogate model was based on the conditions and dimensions of an area with a specific groundwater conservation program, the exact thresholds identified in this study may not translate to other aquifer systems and should be viewed in the context of this study, which is to identify how lagged processes influence groundwater conservation initiatives. However, regardless of the specific thresholds, we would expect the general relationships among variables to be consistent (e.g., lagged changes in recharge become more important in settings with greater vertical hydraulic conductivity).

Second, the applied pumping and deep percolation rates are based on statistical relationships using limited data. While Kansas has the most robust pumping well metering data in the United States (Foster et al., 2020; USDA National Agricultural Statistics Service, 2019), pumping rates for the period from 1955 to 1992 are based on a regression model while rates from 1993 to 2019 are based on observed data. Additionally, when developing the projected pumping rates, we assumed that irrigation efficiency does not change and that neither the conservation nor the non-conservation areas change their pumping practices, which may not be the case as new technologies are adopted by or groundwater resources begin to become less accessible to the agricultural community. Applied deep percolation rates were developed using 10 years of modeled data and extrapolated to fill the historical record, which may have resulted in deep percolation rates that are too high. We also assumed that the (transect-perpendicular) east-to-west LIs to the system are constant through time. These issues point to a critical need to better monitor vertical fluxes of water in deep vadose zones and lateral fluxes in aquifers to inform future modeling efforts and conservation program evaluations.

Third, the use of the UZF package to simulate variably saturated flow is limited in several aspects. If applied deep percolation rates are greater than the prescribed saturated hydraulic conductivity, excess water is removed from the system, as low hydraulic conductivity conditions typical of lateral-flow-dominated cases are limited not just by the rate at which water percolates through the unsaturated zone, but also by the supply of water able to infiltrate into the root zone. Incorporating heterogeneity into the model domain was not possible with the UZF package as it can only be applied to one active layer, further simplifying the representation. We had attempted to address this limitation by using another MODFLOW-based variably-saturated flow solution, HYDRUS Package for MODFLOW (Beegum et al., 2018; Seo et al., 2007), which solves a 1-D unsaturated Richards Equation for each cell column, but experienced both instability and anomalous results that prevented its application here. Finally, all projection results are based on randomly sampling the historical record of precipitation to generate time series for deep percolation and pumping, which provides realistic daily meteorological dynamics but inherently ignores climate change impacts and implications.

Although our modeling approach may disregard some locally important heterogeneity, our objective was to analyze the major factors controlling the long-term effectiveness of groundwater conservation initiatives. Our simplified surrogate modeling approach allows for the fundamental processes to be investigated while removing the impact of site specific phenomena, ultimately allowing for a more generalized understanding of aquifer system dynamics that can be transferred to other aquifers that are at risk of depletion. Applying these assumptions, we were able to investigate the interplay among vertical hydraulic conductivity, soil water retention properties, lateral flows, and recharge. This allowed us to assess the long-term effectiveness of pumping reduction based groundwater conservation strategies, and estimate the extension of the usable aquifer lifetime for both the lateral-flow- and recharge-dominated cases.

## 4. Conclusions

Pumping reductions are, in many settings, the only viable method for extending the lifetime of groundwater resources. In this study, we demonstrate that pumping reductions can lead to changes in lateral groundwater flow and recharge, and these lagged responses to pumping reductions ultimately have a substantial influence over the long-term effectiveness of groundwater conservation initiatives. The degree to which lateral flow and recharge impact long-term effectiveness is strongly dependent on the vertical hydraulic conductivity of the unsaturated zone, which controls the degree to which changes in deep percolation can translate into changes in groundwater recharge. We found that larger reductions in pumping result in a longer extension of the usable aquifer lifetime, and that this impact is most strongly felt in the center of the conservation area and that the benefits of groundwater conservation programs may extend beyond the areas implementing conservation practices due to lateral flow. However, we anticipate that the impact of lateral flow will lessen as the size of the conservation area increases and its perimeter-to-area ratio decreases. Thus, this work should be considered an initial step in assessing the interplay between the various mechanisms controlling an aquifer's response to pumping-based conservation initiatives.

## Data Availability Statement

Data and code are available at <https://osf.io/amu9e/>. <https://doi.org/10.17605/osf.io/amu9e> during the review process and will be placed in a repository at the time of paper acceptance.

## Acknowledgments

This work was supported, in part, by the United States Department of Agriculture (USDA) under USDA-NIFA Grant 2018-67003-27406 and subaward RC104693B, the USDA and the National Science Foundation (NSF) under USDA-NIFA/NSF-INFEWS Grant 2018-67003-27406 subaward RC108063UK, and the NSF under Grant No. 2108196. Any opinions, findings, and conclusions or recommendations expressed in this material are those of the authors and do not necessarily reflect the views of the USDA or NSF. We would like to thank Geoff Bohling and Brownie Wilson for their help procuring data and helpful comments.

## References

- Asher, M. J., Croke, B. F. W., Jakeman, A. J., & Peeters, L. J. M. (2015). A review of surrogate models and their application to groundwater modeling. *Water Resources Research*, *51*(8), 5957–5973. <https://doi.org/10.1002/2015WR016967>
- Bailey, R. T., Morway, E. D., Niswonger, R. G., & Gates, T. K. (2013). Modeling variably saturated multispecies reactive groundwater solute transport with MODFLOW-UZF and RT3D. *Groundwater*, *51*(5), 752–761. <https://doi.org/10.1111/j.1745-6584.2012.01009.x>
- Bakker, M., Post, V., Langevin, C. D., Hughes, J. D., White, J. T., Starn, J. J., & Fienen, M. N. (2016). Scripting MODFLOW model development using Python and FloPy. *Groundwater*, *54*(5), 733–739. <https://doi.org/10.1111/gwat.12413>
- Beegun, S., Šimůnek, J., Szymkiewicz, A., Sudheer, K. P., & Nambi, I. M. (2018). Updating the coupling algorithm between HYDRUS and MODFLOW in the HYDRUS package for MODFLOW. *Vadose Zone Journal*, *17*(1), 180034. <https://doi.org/10.2136/vzj2018.02.0034>
- Beven, K. (2006). A manifesto for the equifinality thesis. *The Model Parameter Estimation Experiment*, *320*(1), 18–36. <https://doi.org/10.1016/j.jhydrol.2005.07.007>
- Bierkens, M. F. P., & Wada, Y. (2019). Non-renewable groundwater use and groundwater depletion: A review. *Environmental Research Letters*, *14*(6), 063002. <https://doi.org/10.1088/1748-9326/ab1a5f>
- Brooks, R. H., & Corey, A. T. (1966). Properties of porous media affecting fluid flow. *Journal of the Irrigation and Drainage Division*, *92*(2), 61–90. <https://doi.org/10.1061/jrcea4.0000425>
- Butler, J. J., Jr., Bohling, G. C., Whittemore, D. O., & Wilson, B. B. (2020a). Charting pathways toward sustainability for aquifers supporting irrigated agriculture. *Water Resources Research*, *56*(10), e2020WR027961. <https://doi.org/10.1029/2020WR027961>
- Butler, J. J., Jr., Bohling, G. C., Whittemore, D. O., & Wilson, B. B. (2020b). A roadblock on the path to aquifer sustainability: Underestimating the impact of pumping reductions. *Environmental Research Letters*, *15*(1), 014003. <https://doi.org/10.1088/1748-9326/ab6002>
- Butler, J. J., Jr., Whittemore, D. O., Reboulet, E. C., Knobbe, S., Wilson, B. B., & Bohling, G. C. (2019). High Plains aquifer index well program: 2019 annual report.
- Butler, J. J., Jr., Whittemore, D. O., Wilson, B. B., & Bohling, G. C. (2016). A new approach for assessing the future of aquifers supporting irrigated agriculture. *Geophysical Research Letters*, *43*(5), 2004–2010. <https://doi.org/10.1002/2016GL067879>
- Callegary, J. B., Megdal, S. B., Tapia Villaseñor, E. M., Petersen-Perlman, J. D., Minjárez Sosa, I., Monreal, R., et al. (2018). Findings and lessons learned from the assessment of the Mexico-United States transboundary San Pedro and Santa Cruz aquifers: The utility of social science in applied hydrologic research. *Special Issue on International Shared Aquifer Resources Assessment and Management*, *20*, 60–73. <https://doi.org/10.1016/j.ejrh.2018.08.002>
- Castilla-Rho, J. C., Rojas, R., Andersen, M. S., Holley, C., & Mariethoz, G. (2019). Sustainable groundwater management: How long and what will it take? *Global Environmental Change*, *58*, 101972. <https://doi.org/10.1016/j.gloenvcha.2019.101972>
- Deines, J. M., Kendall, A. D., Butler, J. J., Jr., Basso, B., & Hyndman, D. W. (2021). Combining remote sensing and crop models to assess the sustainability of stakeholder-driven groundwater management in the US High Plains aquifer. *Water Resources Research*, e2020WR027756. <https://doi.org/10.1029/2020WR027756>
- Deines, J. M., Kendall, A. D., Butler, J. J., Jr., & Hyndman, D. W. (2019). Quantifying irrigation adaptation strategies in response to stakeholder-driven groundwater management in the US High Plains aquifer. *Environmental Research Letters*, *14*(4), 044014. <https://doi.org/10.1088/1748-9326/aafe39>
- Deines, J. M., Schipanski, M. E., Golden, B., Zipper, S. C., Nozari, S., Rottler, C., et al. (2020). Transitions from irrigated to dryland agriculture in the Ogallala Aquifer: Land use suitability and regional economic impacts. *Agricultural Water Management*, *233*, 106061. <https://doi.org/10.1016/j.agwat.2020.106061>
- DeSimone, L. A., McMahon, P. B., & Rosen, M. R. (2015). The quality of our nation's waters: Water quality in principal aquifers of the United States, 1991-2010 (Report No. 1360) (p. 161). <https://doi.org/10.3133/cir1360>
- Dieter, C. A., Maupin, M. A., Caldwell, R. R., Harris, M. A., Ivahnenko, T. I., Lovelace, J. K., et al. (2018). Estimated use of water in the United States in 2015 (Report No. 1441) (p. 76). <https://doi.org/10.3133/cir1441>
- Doherty, J. (2015). *Calibration and uncertainty analysis for complex environmental models*. Watermark Numerical Computing Brisbane.

- Foster, T., Brozović, N., & Butler, A. P. (2017). Effects of initial aquifer conditions on economic benefits from groundwater conservation. *Water Resources Research*, 53(1), 744–762. <https://doi.org/10.1002/2016WR019365>
- Foster, T., Mieno, T., & Brozović, N. (2020). Satellite-based monitoring of irrigation water use: Assessing measurement errors and their implications for agricultural water management policy. *Water Resources Research*, 56(11), e2020WR028378. <https://doi.org/10.1029/2020WR028378>
- Fross, D., Sophocleous, M. A., Wilson, B. B., & Butler, J. J., Jr. (2012). *Kansas High Plains aquifer Atlas*. Kansas Geological Survey. Retrieved from [http://www.kgs.ku.edu/HighPlains/HPA\\_Atlas/index.html](http://www.kgs.ku.edu/HighPlains/HPA_Atlas/index.html)
- Gleeson, T., Alley, W. M., Allen, D. M., Sophocleous, M. A., Zhou, Y., Taniguchi, M., & VanderSteen, J. (2012). Towards sustainable groundwater use: Setting long-term goals, backcasting, and managing adaptively. *Ground Water*, 50(1), 19–26. <https://doi.org/10.1111/j.1745-6584.2011.00825.x>
- Gleeson, T., Cuthbert, M., Ferguson, G., & Perrone, D. (2020). Global groundwater sustainability, resources, and systems in the anthropocene. *Annual Review of Earth and Planetary Sciences*, 48(1), 431–463. <https://doi.org/10.1146/annurev-earth-071719-055251>
- Golden, B. (2018). Monitoring the impacts of Sheridan County 6 local enhanced management area: Final report for 2013 – 2017. Retrieved from [https://agriculture.ks.gov/docs/default-source/dwr-water-appropriation-%20documents/sheridancounty6\\_lemma\\_goldenreport\\_2013-2017.pdf?sfvrsn=dac48ac1\\_0](https://agriculture.ks.gov/docs/default-source/dwr-water-appropriation-%20documents/sheridancounty6_lemma_goldenreport_2013-2017.pdf?sfvrsn=dac48ac1_0)
- Gurdak, J. J., Walvoord, M. A., & McMahon, P. B. (2008). Susceptibility to enhanced chemical migration from depression-focused preferential flow, High Plains aquifer. *Vadose Zone Journal*, 7(4), 1218–1230. <https://doi.org/10.2136/vzj2007.0145>
- Hansen, C. V. (1991). Estimates of freshwater storage and potential natural recharge for principal aquifers in Kansas (Report No. 87–4230). <https://doi.org/10.3133/wri874230>
- Hou, X., Wang, S., Jin, X., Li, M., Lv, M., & Feng, W. (2020). Using an ETWatch (RS)-UZf-MODFLOW coupled model to optimize joint use of transferred water and local water sources in a saline water area of the north China plain. *Water*, 12(12), 3361. <https://doi.org/10.3390/w12123361>
- Hu, Y., Moiwu, J. P., Yang, Y., Han, S., & Yang, Y. (2010). Agricultural water-saving and sustainable groundwater management in shijiazhuang irrigation district, north China plain. *Journal of Hydrology*, 393(3), 219–232. <https://doi.org/10.1016/j.jhydrol.2010.08.017>
- Huggins, X., Gleeson, T., Kumm, M., Zipper, S. C., Wada, Y., Troy, T. J., & Famiglietti, J. S. (2022). Hotspots for social and ecological impacts from freshwater stress and storage loss. *Nature Communications*, 13(1), 439. <https://doi.org/10.1038/s41467-022-28029-w>
- Hunt, R. J., Prudic, D. E., Walker, J. F., & Anderson, M. P. (2008). Importance of unsaturated zone flow for simulating recharge in a humid climate. *Groundwater*, 46(4), 551–560. <https://doi.org/10.1111/j.1745-6584.2007.00427.x>
- Kansas Department of Agriculture (2013). Order of designation approving the Sheridan 6 local enhanced management area within groundwater management district No. 4. Retrieved from <https://sftp.kda.ks.gov:4443/LEMAs/SD6/OrderOfDesignation.2013%200417.pdf>
- Kansas Department of Agriculture (2018). Order of designation regarding the groundwater management district No. 4 district wide local enhanced management plan. Retrieved from [https://agriculture.ks.gov/docs/default-source/dwr-water-appropriation-documents/gmd4\\_lemma\\_orderofdesignation.pdf?sfvrsn=30e981c1\\_4](https://agriculture.ks.gov/docs/default-source/dwr-water-appropriation-documents/gmd4_lemma_orderofdesignation.pdf?sfvrsn=30e981c1_4)
- Kansas Department of Agriculture (2021). Order of designation regarding the management plan for the Wichita County local enhanced management area. Retrieved from [https://agriculture.ks.gov/docs/default-source/dwr-water-appropriation-documents/whc-lemma-order-of-designation--final.pdf?sfvrsn=60d690c1\\_0](https://agriculture.ks.gov/docs/default-source/dwr-water-appropriation-documents/whc-lemma-order-of-designation--final.pdf?sfvrsn=60d690c1_0)
- Kansas Statutes Annotated 82a-1041. (2012). Local enhanced management areas; establishment procedures; duties of chief engineer. hearing; notice; orders; review Retrieved from [http://www.ksrevisor.org/statutes/chapters/ch82a/082a\\_010\\_0041.html](http://www.ksrevisor.org/statutes/chapters/ch82a/082a_010_0041.html)
- Katz, B. S., Stotler, R. L., Hirmas, D., Ludvigson, G., Smith, J. J., & Whittemore, D. O. (2016). Geochemical recharge estimation and the effects of a declining water table. *Vadose Zone Journal*, 15(vzj2016). <https://doi.org/10.2136/vzj2016.04.0031>
- Kennedy, J., Ferré, T. P. A., & Creutzfeldt, B. (2016). Time-lapse gravity data for monitoring and modeling artificial recharge through a thick unsaturated zone. *Water Resources Research*, 52(9), 7244–7261. <https://doi.org/10.1002/2016WR018770>
- Kling, H., Fuchs, M., & Paulin, M. (2012). Runoff conditions in the upper Danube basin under an ensemble of climate change scenarios. *Journal of Hydrology*, 424(425), 264–277. <https://doi.org/10.1016/j.jhydrol.2012.01.011>
- Knoben, W. J. M., Freer, J. E., & Woods, R. A. (2019). Technical note: Inherent benchmark or not? Comparing Nash-Sutcliffe and Kling-Gupta efficiency scores. *Hydrology and Earth System Sciences*, 23(10), 4323–4331. <https://doi.org/10.5194/hess-23-4323-2019>
- Konikow, L. F., & Bredehoeft, J. D. (1992). Ground-water models cannot be validated. *Validation of Geo-Hydrological Models Part 1*, 15(1), 75–83. [https://doi.org/10.1016/0309-1708\(92\)90033-X](https://doi.org/10.1016/0309-1708(92)90033-X)
- Lee, E., Jayakumar, R., Shrestha, S., & Han, Z. (2018). Assessment of transboundary aquifer resources in Asia: Status and progress towards sustainable groundwater management. *Special Issue on International Shared Aquifer Resources Assessment and Management*, 20, 103–115. <https://doi.org/10.1016/j.ejrh.2018.01.004>
- Lin, X., Harrington, J., Ciampitti, I., Gowda, P., Brown, D., & Kisekka, I. (2017). Kansas trends and changes in temperature, precipitation, drought, and frost-free days from the 1890s to 2015. *Journal of Contemporary Water Research & Education*, 162(1), 18–30. <https://doi.org/10.1111/j.1936-704X.2017.03257.x>
- Lipponen, A., & Chilton, J. (2018). Development of cooperation on managing transboundary groundwaters in the pan-European region: The role of international frameworks and joint assessments. *Special Issue on International Shared Aquifer Resources Assessment and Management*, 20, 145–157. <https://doi.org/10.1016/j.ejrh.2018.05.001>
- Liu, G., Wilson, B. B., Bohling, G. C., Whittemore, D. O., & Butler, J. J., Jr. (2022). Estimation of specific yield for regional groundwater models: Pitfalls, ramifications, and a promising path forward. *Water Resources Research*, 58(1), e2021WR030761. <https://doi.org/10.1029/2021WR030761>
- McKay, M. D., Beckman, R. J., & Conover, W. J. (1979). Comparison of three methods for selecting values of input variables in the analysis of output from a computer code. *Technometrics*, 21(2), 239–245. <https://doi.org/10.1080/00401706.1979.10489755>
- McMahon, P. B., Dennehy, K. F., Bruce, B. W., Böhlke, J. K., Michel, R. L., Gurdak, J. J., & Hurlbut, D. B. (2006). Storage and transit time of chemicals in thick unsaturated zones under rangeland and irrigated cropland, High Plains, United States. *Water Resources Research*, 42(3). <https://doi.org/10.1029/2005WR004417>
- Miro, M. E., & Famiglietti, J. S. (2019). A framework for quantifying sustainable yield under California's Sustainable Groundwater Management Act (SGMA). *Sustainable Water Resources Management*, 5(3), 1165–1177.
- Morway, E. D., Niswonger, R. G., Langevin, C. D., Bailey, R. T., & Healy, R. W. (2013). Modeling variably saturated subsurface solute transport with MODFLOW-UZF and MT3DMS. *Groundwater*, 51(2), 237–251. <https://doi.org/10.1111/j.1745-6584.2012.00971.x>
- Nazarieh, F., Ansari, H., Ziaei, A. N., Izady, A., Davari, K., & Brunner, P. (2018). Spatial and temporal dynamics of deep percolation, lag time and recharge in an irrigated semi-arid region. *Hydrogeology Journal*, 26(7), 2507–2520. <https://doi.org/10.1007/s10040-018-1789-z>

- Niswonger, R. G., & Prudic, D. E. (2009). Comment on “evaluating interactions between groundwater and vadose zone using the HYDRUS-based flow package for MODFLOW” by Navin Kumar C. Twarakavi, Jirka Šimůnek, and sophia Seo. *Vadose Zone Journal*, 8(3), 818–819. <https://doi.org/10.2136/vzj2008.0155>
- Niswonger, R. G., Prudic, D. E., & Regan, R. S. (2006). Documentation of the unsaturated-zone flow (UZFI) package for modeling unsaturated flow between the land surface and the water table with MODFLOW-2005 (Report No. 6-A19). <https://doi.org/10.3133/tm6A19>
- Pauloo, R. A., Fogg, G. E., Guo, Z., & Harter, T. (2021). Anthropogenic basin closure and groundwater salinization (ABCSAL). *Journal of Hydrology*, 593, 125787. <https://doi.org/10.1016/j.jhydrol.2020.125787>
- Pfeiffer, L., & Lin, C.-Y. C. (2010). The effect of irrigation technology on groundwater use. *Choice*, 25(3), 1–6.
- Poeter, E. P., & Hill, M. C. (1999). UCODE, a computer code for universal inverse modeling. *Computers & Geosciences*, 25(4), 457–462. [https://doi.org/10.1016/s0098-3004\(98\)00149-6](https://doi.org/10.1016/s0098-3004(98)00149-6)
- Razavi, S., Tolson, B. A., & Burn, D. H. (2012). Review of surrogate modeling in water resources. *Water Resources Research*, 48(7). <https://doi.org/10.1029/2011WR011527>
- Rogers, D. H., & Lamm, F. R. (2012). Kansas irrigation trends. In *Presented at the proceedings of the 24th annual central Plains irrigation Conference, Colby, Kansas*. Central Plains Irrigation Association.
- Savenije, H. H. G. (2001). Equifinality, a blessing in disguise? *Hydrological Processes*, 15(14), 2835–2838. <https://doi.org/10.1002/hyp.494>
- Scanlon, B. R., Faunt, C. C., Longueuevegne, L., Reedy, R. C., Alley, W. M., McGuire, V. L., & McMahon, P. B. (2012). Groundwater depletion and sustainability of irrigation in the US High Plains and central valley. *Proceedings of the National Academy of Sciences*, 109(24), 9320–9325. <https://doi.org/10.1073/pnas.1200311109>
- Scanlon, B. R., Keese, K. E., Flint, A. L., Flint, L. E., Gaye, C. B., Edmunds, W. M., & Simmers, I. (2006). Global synthesis of groundwater recharge in semiarid and arid regions. *Hydrological Processes*, 20(15), 3335–3370. <https://doi.org/10.1002/hyp.6335>
- Seo, H. S., Simunek, J., & Poeter, E. P. (2007). *Documentation of the HYDRUS package for -2000, the US geological survey modular ground-water model*. IGWMC-International Ground Water Modeling Center.
- Sindico, F., Hirata, R., & Manganeli, A. (2018). The Guarani Aquifer System: From a Beacon of hope to a question mark in the governance of transboundary aquifers. *Special Issue on International Shared Aquifer Resources Assessment and Management*, 20, 49–59. <https://doi.org/10.1016/j.ejrh.2018.04.008>
- Smith, R. (1983). Approximate soil water movement by kinematic characteristics. *Soil Science Society of America Journal*, 47(1), 3–8. <https://doi.org/10.2136/sssaj1983.03615995004700010001x>
- Smith, R., & Hebbert, R. H. B. (1983). Mathematical simulation of interdependent surface and subsurface hydrologic processes. *Water Resources Research*, 19(4), 987–1001. <https://doi.org/10.1029/WR019i004p00987>
- USDA National Agricultural Statistics Service. (2019). 2018 Irrigation and water management survey, 3. Retrieved from [https://www.nass.usda.gov/Publications/AgCensus/2017/Online\\_Resources/Farm\\_and\\_Ranch\\_Irrigation\\_Survey/fris.pdf](https://www.nass.usda.gov/Publications/AgCensus/2017/Online_Resources/Farm_and_Ranch_Irrigation_Survey/fris.pdf)
- Voss, C. I. (2011a). Editor’s message: Groundwater modeling fantasies—Part 1, adrift in the details. *Hydrogeology Journal*, 19(7), 1281–1284. <https://doi.org/10.1007/s10040-011-0789-z>
- Voss, C. I. (2011b). Editor’s message: Groundwater modeling fantasies—Part 2, down to Earth. *Hydrogeology Journal*, 19(8), 1455–1458. <https://doi.org/10.1007/s10040-011-0790-6>
- Whittemore, D. O., Butler, J. J., Jr., & Wilson, B. B. (2018). *Status of the High Plains aquifer in Kansas* (Vol. 22). Kansas Geological Survey Technical Series. Retrieved from [www.kgs.ku.edu/Publications/Bulletins/TS22/index.html](http://www.kgs.ku.edu/Publications/Bulletins/TS22/index.html)
- Wilson, B. B., Liu, G., Bohling, G. C., & Butler, J. J., Jr. (2021). GMD4 groundwater flow model: High Plains aquifer modeling maintenance project (Report No. 2021-6). Retrieved from <https://www.kgs.ku.edu/Publications/OFR/2021/OFR2021-6.pdf>
- Zell, W. O., & Sanford, W. E. (2020). Calibrated simulation of the long-term average surficial groundwater system and derived spatial distributions of its characteristics for the contiguous United States. *Water Resources Research*, 56(8), e2019WR026724. <https://doi.org/10.1029/2019WR026724>
- Zipper, S. C., Gleeson, T., Kerr, B., Howard, J. K., Rohde, M. M., Carah, J., & Zimmerman, J. (2019). Rapid and accurate estimates of streamflow depletion caused by groundwater pumping using analytical depletion functions. *Water Resources Research*, 55(7), 5807–5829. <https://doi.org/10.1029/2018WR024403>
- Zipper, S. C., Lamontagne-Hallé, P., McKenzie, J. M., & Rocha, A. V. (2018). Groundwater controls on postfire permafrost thaw: Water and energy balance effects. *Journal of Geophysical Research: Earth Surface*, 123(10), 2677–2694. <https://doi.org/10.1029/2018JF004611>
- Zipper, S. C., Soylu, M. E., Kucharik, C. J., S. P. L., II, & Loheide II, S. P. (2017). Quantifying indirect groundwater-mediated effects of urbanization on agroecosystem productivity using MODFLOW-AgroIBIS (MAGI), a complete critical zone model. *Ecological Modelling*, 359, 201–219. <https://doi.org/10.1016/j.ecolmodel.2017.06.002>

## References From the Supporting Information

- Abatzoglou, J. T. (2013). Development of gridded surface meteorological data for ecological applications and modelling. *International Journal of Climatology*, 33(1), 121–131. <https://doi.org/10.1002/joc.3413>